Progress In Electromagnetics Research B, Vol. 53, 47–71, 2013

WIDE-BAND SECURE COMPRESSED SPECTRUM SENSING FOR COGNITIVE RADIO SYSTEMS

Mostafa El-Khamy[1, *], Mohammed Farrag[2], and Mohamed El-Sharkawy[3]

[1]Electrical Engineering Department, Faculty of Engineering, Alexandria University, Alexandria 21544, Egypt

[2]Department of Electronics and Communications Engineering, Egypt-Japan University for Science and Technology (E-JUST), Borg El-Arab, Alexandria, Egypt

[3]Purdue School of Engineering and Technology, IUPUI, Indianapolis, USA

Abstract—Cooperative wide-band spectrum sensing has been considered to enable cognitive radio operation of wireless regional area networks (WRAN) in the UHF and VHF TV broadcasting bands. In this paper, cooperative compressed spectrum sensing is considered to enable fast sensing of the wide-band spectrum. The speed and accuracy of spectrum sensing are improved by further optimization of the compressed sensing receiver, which is done blindly without any prior knowledge of the sensed signal. Enhanced compressed spectrum sensing algorithms are proposed for the cases of individual spectrum sensing and cooperative spectrum sensing. The cooperative signal reconstruction process is modified to optimally combine the received measurements at the fusion center. A low complexity authentication mechanism, which is inherent to cooperative compressed spectrum sensing, is proposed to make the cognitive radio system immune to adversary attacks.

1. INTRODUCTION

Cognitive radio (CR) technology has the potential to alleviate the scarcity of wireless spectrum by allowing the next generations of wireless devices to utilize the white spaces in the wireless spectrum. CR

Received 18 May 2013, Accepted 6 July 2013, Scheduled 8 July 2013

* Corresponding author: Mostafa El-Khamy (m_elkhamy@ieee.org).

allows a secondary user to reuse a wireless spectrum band as long as its licensed user is protected against harmful interference [1, 2]. The IEEE 802.22 wireless regional area network (WRAN) standard [3] allows WRAN systems to utilize channels in the UHF and VHF bands in the frequency range from 54 MHz to 862 MHz, as long as they do not interfere with licensed broadcast incumbent services on these bands, such as wireless microphones and TV broadcasting services. WRAN systems should also be capable of dynamic frequency selection due to the fragmented and time-varying spectrum capability in the specified TV broadcasting band. Hence, WRAN terminals should be equipped with cognitive radio features for real-time sensing of this wide-band spectrum and quick detection of any activity by an incumbent primary user (PU) or other WRAN terminals on the channels of interest. To aid in frequency selection, the spectrum sensing information can be used jointly with geolocation databases to decide on the local vacant channels, the WRAN transmission band and power.

Spectrum sensing is challenging due to the requirements set by the FCC on the sensing speed and accuracy [4]. This is particularly manifested in wide-band systems due to the high sampling rates required, which means complex and expensive hardware with high power consumption. Conventional wide-band spectrum sensing techniques include successive scanning of multiple frequency bands through tunable band-bass filters [5, 6]. This technique is not very attractive due to its extensive RF hardware, and may fail to scan all the bands with the desired speed. Another approach to wide-band spectrum sensing is to search the multiple frequency bands simultaneously by deploying a wide-band RF front-end together with high-speed signal processing architectures [7]. However, the high sampling rate, which is at least the Nyquist rate or twice the bandwidth, required for conventional spectrum estimation of a wide-band signal poses a major practical challenge to the deployment of this technique. Also, the timing requirements for rapid sensing may only allow for acquisition of a small number of samples, which may not provide sufficient statistics when conventional signal reconstruction methods are used.

Compressed sensing (CS) allows sensing of sparse signals at sub-Nyquist sampling rates, and their reliable signal recovery via computationally efficient algorithms [8–10]. CS states that a signal can be recovered from a small number of projections over a sensing basis (measurements) if it is sparse over a representation basis that is incoherent with the sensing basis. The minimum number of measurements required for reliable signal recovery depends on the sparsity of the signal representation with the sparsifying basis. In

the context of image and audio compression, it has been shown that CS recovery can be made more efficient by adopting a tree-structured dictionary of orthogonal bases adapted to the measured signal [11]. CS has also been successfully deployed in track-before-detect radar systems, which reconstruct the whole radar scene from sparse measurements [12]. Also using CS, low-cost high-quality sparse array 3-D microwave imaging have recently been shown to be feasible [13].

Compressed spectrum sensing (CSS) is an attractive solution for wide-band spectrum sensing [14–16]. In a two-step CS approach, the sparsity order of the wide spectrum is quickly estimated using a small number of samples at the first step, then the total number of samples collected is adjusted according to the estimated signal sparsity order at the second step [17]. Wavelet edge detection can be utilized to improve CS performance, where the wide-band spectrum is viewed as sub-bands, and the detected spectrum edges indicate a change in spectrum occupancy [14, 18].

In cooperative spectrum sensing, several CR terminals sense the spectrum and cooperate to decide on the availability of the CR channels. By exploiting spatial diversity, cooperative sensing helps mitigate hidden-node problems and improve the detection performance at low SNRs [19]. Cooperative sensing can be centralized, where a common control channel is assigned to CR terminals to report their local sensing data to the fusion center (FC), which in turn makes a global decision on the spectrum availability [20]. In distributed cooperative spectrum sensing, the CR terminals share their sensing decisions with other nodes to reach a global decision [21]. CS can be deployed with cooperative sensing, where compressed measurements from multiple sensing terminals are sent to the FC to reconstruct an estimate of the received signal [22]. Security poses a major challenge to cooperative sensing, where greedy secondary users may attack the CR system to selfishly utilize the vacant spectrum, and malicious users may attack to degrade the PU and CR system performance. In such attacks, malicious nodes may report false measurements to the FC to force it to make wrong decisions [23–25].

In this paper, we propose enhanced techniques for compressed spectrum sensing of wide-band signals in the TV broadcasting band to provide higher secondary user throughput and better incumbent user protection. We develop blindly-optimized CS receivers for both individual and centralized cooperative spectrum sensing systems. Coifman and Wickerhauser (CW) optimization [26] with an entropy cost function is deployed to find the optimum basis from a wavelet packet dictionary. This optimization requires knowledge of the

measured signal. However, in WRAN systems, the received signal is unknown since it can be from TV broadcasting services, or wireless microphones, or other WRAN users. Hence, our proposed CS techniques blindly optimize the sparsifying basis without any prior knowledge about the characteristics of the measured signal. Our proposed spectrum sensing techniques improve PU detection probabilities at given false alarm probabilities. To enhance the security of the proposed cooperative CSS system and protect the PU and SUs against malicious attacks, we propose an authentication technique at the WRAN base station (or fusion center), which is inherent to the cooperative CSS algorithm, and can successfully discard false measurements from terminals prior to incorporating them in the signal reconstruction and decision-making processes. The following abbreviations will be used for the algorithms investigated in this paper, CS for compressed sensing, CSS for compressed spectrum sensing, CCSS for cooperative CSS, GOCS for genie-aided optimized CS, GOCCS for genie-aided optimized CCSS, BOCS for blindly optimized CS, BOCCS for blindly optimized CCSS, and SBOCCS for secure BOCCS.

The rest of this paper is organized as follows. In Section 2, the spectrum sensing system model is described. In Section 3, the tools deployed in this paper for individual and cooperative CSS and reconstruction are described. The proposed genie-aided and blindly optimized CSS algorithms are described and analyzed in Sections 4 and 5, respectively. The proposed authentication algorithm for secure CCSS is described and analyzed in Section 6. Section 7 concludes the paper with some discussions.

2. COGNITIVE RADIO SPECTRUM SENSING MODEL

In this section, we describe the system model used to develop the algorithms described in this paper.

2.1. Spectrum Sensing Model

Consider a CR system with J spectrum sensing terminals. The PU signal received at a spectrum sensing terminal j at time index t can be described by

$$\mathbf{r}_j(t) = \begin{cases} \mathbf{h}_j(t)\mathbf{x}(t) + \mathbf{n}_j(t); & \text{PU is active} \\ \mathbf{n}_j(t); & \text{PU is idle} \end{cases}, \tag{1}$$

where $\mathbf{x}$ is the transmitted PU wide-band signal, $\mathbf{n}_j$ the zero-mean wide-band additive white Gaussian noise (AWGN) at secondary user

SU j with variance σ_n^2, and $\mathbf{h}_j$ the complex channel gain for the channel between the PU and SU j, which is normalized to unity for static AWGN channels.

For individual spectrum sensing, the outcome of the spectrum sensing process at the jth terminal is a decision on one of two hypotheses for each PU channel p;

$$\mathcal{H}_j(p) = \begin{cases} \mathcal{H}_1; & \text{PU is active on sub-band } p, \\ \mathcal{H}_0; & \text{PU is idle on sub-band } p. \end{cases} \tag{2}$$

For cooperative sensing with decision fusion, each sensing terminal transmits its decision $\mathcal{H}_j(p)$ to the FC which decides on the global decision $\mathcal{H}(p)$ for each sub-band, using a majority vote or a similar criterion. For cooperative sensing with data fusion, all SUs transmit their raw measurements to the FC which makes a global decision $\mathcal{H}(p)$ about the PU activity on channel p. In this paper, we focus on data fusion systems since they have better performance than decision fusion systems, and have the advantage of shifting the computational complexity from the low-power sensing nodes to the FC. Whereas the sampling rates of the PU signal should be at least the Nyquist rate for conventional spectrum sensing, the PU signal can be sampled at sub-Nyquist sampling rates with CSS. Sub-Nyquist sampling can be done by an analog-to-information converter [27]. An analog-to-information converter maps a continuous time signal to a discrete sequence of measurements. Hence, it can be modeled as two cascaded blocks; an analog to digital converter operating at the Nyquist rate, followed by a compressed sensing block.

Let $\mathbf{y}_j$ be the vector of measurements obtained from sampling $\mathbf{r}_j(t)$ by SU j. An estimate of the PU signal is reconstructed at SU j in case of individual CSS, or at the FC, after observing all J measurements, in case of CCSS. Let $\hat{\mathbf{x}}$ denote the reconstructed estimate of the sensed signal, and $\widehat{\mathbb{S}}_{\mathbf{x}}$ denote its estimated power spectral density (PSD). An energy detector can be used to accumulate the energy $E_p = \sum_{i \in \text{sub-band } p} \widehat{\mathbb{S}}_{\mathbf{x}}(i)$ received in sub-band p. The FC decides on the availability of channel p by the hypotheses

$$\mathcal{H}(p) = \begin{cases} \mathcal{H}_1; & E_p \geq \tau \\ \mathcal{H}_0; & E_p < \tau. \end{cases} \tag{3}$$

The threshold τ is a design parameter and can be empirically set to achieve a certain target false alarm probability (FAP) which is defined by

$$P_{\mathcal{F}} = \mathrm{P}\left\{\mathcal{H}(p) = H_1 \mid \text{PU is idle on sub-band } p\right\}.$$

A false alarm is not desired as it will prevent the secondary user from utilizing a vacant band. The detection probability $P_{\mathcal{D}}$ is the probability

of correctly identifying that the PU is active whenever it is active,

$$P_{\mathcal{D}} = \mathrm{P}\left\{\mathcal{H}(p) = H_1 \mid \text{PU is active on sub-band } p\right\}.$$

The choice of τ provides a trade-off between maximizing the secondary user throughput (by decreasing $P_{\mathcal{F}}$), and minimizing interference to the PU (maximizing $P_{\mathcal{D}}$). A larger τ would result in a lower false alarm probability at the expense of a lower detection probability. On the other hand, if τ is set to be very small, then energy due to noise can be falsely detected, resulting in a $P_{\mathcal{F}}$ of unity, as well as a $P_{\mathcal{D}}$ of unity due to the detection of PU signals with very low received powers. Practical CR systems should operate with a false alarm probability less than 0.1 [1, 2]. The tradeoff between the false alarm and detection probabilities is best characterized by the receiver operating characteristics (ROC) curve, where a better spectrum sensing system will yield higher detection probability at a given false alarm proability.

2.2. Simulation System Model

To evaluate the performance of the proposed spectrum sensing algorithms, a system model compatible with the WRAN system is assumed. It is assumed that that the CR terminals would like to utilize $N_p = 8$ non-overlapping sub-bands, or TV channels, within the band from 75 MHz to 600 MHz, when not occupied by the incumbent signals. This wide band is within the limits specified by the WRAN standard [3], which also specifies that the selected N_p channels may be determined by the sensing terminals from the WRAN geolocation database. Each sub-band or TV channel is assumed to have an 8 MHz bandwidth. To determine the availability of the desired bands, spectrum sensing of the 75–600 MHz wide-band spectrum is performed. Slightly similar models have been adopted in previous works [16, 18].

For Monte-Carlo simulations, the carrier frequencies of the N_p channels are randomly varied in the sensed frequency band. To average the detection performance over cases when the bands are either occupied or available, it is assumed that only 4 of the 8 channels are occupied by the incumbent user at any given time. For realistic performance averaging over different PU received powers, the spectrum sensing terminals receive the PU signals with different signal to noise ratios (SNRs) on the occupied channels.

The sensed signal is measured according to the desired compression ratio (m/N), where m is the number of measurements and N is the number of discrete samples of the measured signal when sampled at the Nyquist rate. The availability of a specific channel can be determined from $\widehat{\mathbb{S}}_{\mathbf{x}}$ by energy detection, c.f., (2), where the

decision threshold τ is determined by the target $P_{\mathcal{F}}$ using Monte-Carlo simulations.

3. COMPRESSED SPECTRUM SENSING (CSS)

In this section, we describe the theory of compressed sensing for individual and cooperative sensing.

3.1. Individual Compressed Spectrum Sensing

Let $\mathbf{y} = \Phi\mathbf{r}$ be a vector of m measurements of an N point sampled received vector $\mathbf{r} = \mathbf{x} + \mathbf{n}$, where Φ is the $m \times N$ measurement matrix. Suppose $\mathbf{r}$ can be represented by a sparse representation $\mathbf{s}$ using a sparsifying transform Ψ. The measurement vector is expressed as

$$\mathbf{y} = \Phi\mathbf{r} = \Phi\Psi\mathbf{s} = \Theta\mathbf{s}. \tag{4}$$

With high probability, $\mathbf{r}$ can be perfectly reconstructed from $\mathbf{y}$ if, for a positive constant c [9]

$$m \geq c\ \mu^2(\Phi, \Psi)\ S\ \log n, \tag{5}$$

where $\mu(\Phi, \Psi) = \sqrt{n}\max_{1\leq m,j\leq n} |\langle \phi_m, \psi_j \rangle|$ is the coherence between the sensing and sparsifying (representation) bases, and $S = \mathcal{S}(\mathbf{s})$ is the maximum number of nonzero elements of $\mathbf{s}$. It has been shown that if the elements of Φ are drawn independently and identically from a Gaussian distribution with zero mean, then with high probability, this random orthonormal basis would have minimal coherence with any fixed sparsifying basis Ψ [9]. In conventional CSS, Ψ is a fixed sparsifying transform, such as the wavelet transform or full wavelet packet (FWP) transform, which is independent of the measured signal.

An estimate of the sparse vector $\hat{\mathbf{s}}$, and hence $\hat{\mathbf{x}}$, is reconstructed by solving the following l_1-norm minimization problem

$$\hat{\mathbf{s}} = \arg_{\mathbf{s}'} \min \left\|\mathbf{s}'\right\|_1 \quad \text{such that} \quad \mathbf{y} = \Phi\Psi\mathbf{s}', \tag{6}$$

where $\|\mathbf{s}'\|_1$ is the l_1-norm of $\mathbf{s}'$. This optimization problem can be efficiently solved by greedy algorithms such as the orthogonal matching pursuit (OMP) algorithm. Hence, the reconstruction process by applying OMP to solve (6) will be denoted $\hat{\mathbf{x}} = \text{OMP}(\mathbf{y}, \Phi, \Psi)$.

3.2. Cooperative Compressed Spectrum Sensing (CCSS)

In case of CCSS with data fusion, each CR node senses its received PU signal $\mathbf{r}_j(t)$ and sends its measurement vector $\mathbf{y}_j$ to the FC. To recover the PU signal, greedy pursuit algorithms, such as the simultaneous

orthogonal matching pursuit (SOMP) algorithm, could be used [18, 28]. The SOMP algorithm exploits the common sparse support among the J measurements [12].

The SOMP algorithm jointly recovers all of the signals from the measurement matrix $\mathbf{Y} = \{\mathbf{y}_1, \mathbf{y}_2, \ldots, \mathbf{y}_J\}$, where $\mathbf{y}_j = \Phi \mathbf{r}_j$, into an $N \times J$ matrix $\hat{\mathbf{X}} = \{\hat{\mathbf{x}}_1, \hat{\mathbf{x}}_2, \ldots, \hat{\mathbf{x}}_J\}$ by $\hat{\mathbf{X}} = \text{SOMP}(\mathbf{Y}, \Phi, \Psi)$. The SOMP algorithm takes as input the $m \times N$ dictionary matrix $\Theta = \Phi\Psi$, whose columns are ϑ_i, and the $m \times J$ measurements matrix $\mathbf{Y}$. The SOMP algorithm requires that the elementary signals be weakly correlated [28], and this is satisfied by having independent basis vectors, through drawing the elements of the measurement matrix independently and identically from a zero-mean Gaussian distribution. The SOMP algorithm is run for a maximum number of iterations T, which depends on the expected sparsity measure S. The output of the SOMP algorithm includes the $m \times J$ approximation matrix A_T and the matrix of the estimated sparse signal $\hat{\mathbf{S}}$, from which the reconstructed signal matrix is calculated as $\hat{\mathbf{X}} = \Psi\hat{\mathbf{S}}$.

With conventional CCSS, the SOMP algorithm assumes a fixed sparsifying basis Ψ, such as the wavelet transform or the full wavelet packet. However, better reconstruction accuracy with the same number of measurements m can be achieved by optimizing the sparsifying basis, as explained in the following sections.

4. GENIE-AIDED OPTIMIZED COMPRESSED SENSING

In case of single user compressed sensing, the sensing performance can be improved by optimization of the sparsifying basis [29, 30]. In this section, we present an optimized CCSS algorithm that can achieve better PU detection than conventional CCSS. PU detection by CSS algorithms improves by increasing the number of measurements, or equivalently the compression ratio m/N. Hence, it is desired to improve the detection performance of CSS at a given false alarm probability and sampling rate. By the condition of (5), perfect reconstruction is possible with a smaller number of measurements if the sparsity measure S of $\mathbf{s}$ is minimized. S, in turn, depends on the choice of the sparsifying basis Ψ.

Whereas conventional CSS uses fixed sparsifying bases which are independent of the measured signal, the proposed technique optimizes the sparsifying basis Ψ to maximize the probability of prefect signal reconstruction at a given sampling rate. We present hypothetical genie-aided optimized CS by optimizing the sparsifying basis Ψ, assuming perfect knowledge of the sensed signal $\mathbf{r}$, to find the optimum basis $\Psi^\star$ that maximizes the sparsity of the representation of the sensed signal,

i.e.,

$$\Psi^{\star} = \arg_{\Psi} \min \mathcal{S}\left(\Psi^{-1}\mathbf{r}\right). \tag{7}$$

Rather than using the full wavelet packet transform, the wavelet packet transform is optimized to the sensed signal, with Shannon entropy as a cost function. The Coifman and Wickerhauser (CW) search strategy [26] is used to search for the optimized wavelet packet (OWP). For a signal $\mathbf{x} = [x_1, x_2, \ldots, x_n]$, let $p_n = |x_n|^2/\|\mathbf{x}\|^2$ be the contribution of the nth coordinate to the energy of $\mathbf{x}$, then the deployed Shannon entropy measure is defined by

$$\mathbb{H} = -\sum_{n} p_n \log p_n. \tag{8}$$

$\mathbb{H}$ is an additive cost function, and it can be shown that minimizing $\mathbb{H}$ maximizes the sparsity (minimizes S) of the sparse vector representation $\mathbf{s}$ (e.g., $\mathbb{H} = 0$ if $S = 1$). This modified Shannon entropy satisfies all characteristics of a "good" sparsity measure [31]. The wavelet packet tree is optimized to minimize a desired cost function, using CW optimization as follows:

Algorithm 1 *Coifman and Wickerhauser Optimization*

Let C_1 be the cost of a non-leaf node, and C_2 be the sum of the costs of its leaves. The optimization process recourses up the tree towards its root such that

i. if $C_1 \leq C_2$, the node is marked as part of the best basis set and any marks of the nodes in the sub-tree of this node are removed.

ii. if $C_1 > C_2$, keep this decomposition and use C_1 as the cost of this parent node and its sub-tree.

When the cost function is the Shannon energy entropy $\mathbb{H}$, then the CW search strategy guarantees that the coefficients collected from the leaves of the optimized wavelet decomposition tree will have the minimum Shannon entropy value, and thus the maximum sparsity. Figure 1 shows an example of the fixed wavelet transform and the full

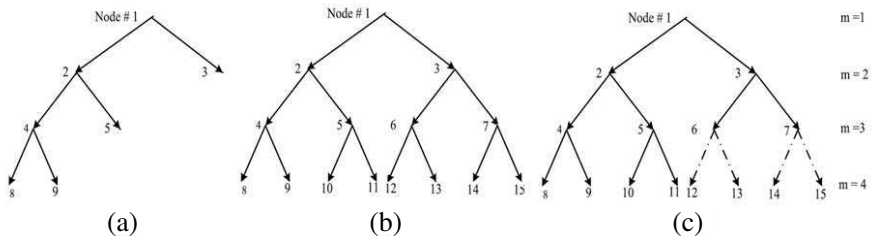

Figure 1. (a) Wavelet transform. (b) Full wavelet packet (FWP) transform. (c) Example of an OWP tree with nodes 1 to 5 decomposed.

wavelet packet transform. It also shows a best basis tree of the OWP transform, where nodes 1 to 5 are decomposed and the remaining nodes are not.

The optimized sparsifying basis $\Psi^\star$ is constructed from the OWP best basis tree as follows:

Algorithm 2 *Optimized Wavelet Packet (OWP) Construction*

Let $L \leq \log_2 N$ be the number of decomposition levels of the OWP, N be the length of the signal to be transformed, and $\mathbf{t}$ be the 2^{L-1} best tree vector. The elements of $\mathbf{t}$ corresponding to the indices of the decomposed nodes are set to ones and the other elements are set to zeros. The OWP matrix is constructed from the OWP tree by

i. Construct the $(N \times N)$ one level wavelet transform matrix W_N from the coefficients of the corresponding wavelet low-pass filter h_0, c.f., [26].

ii. At the mth decomposition level, let the vector $\mathbf{t_m} = \{\mathbf{t}(i)\}_{i=2^{m-1},\ldots,2^m-1}$ represent the decomposition of nodes in the OWP tree at this level.

iii. Let $d = N/2^{m-1}$, and the decomposition matrix D_i be defined as

$$D_i = \begin{cases} W_d, & \text{if } \mathbf{t}_m(i) = 1 \\ I_d, & \text{otherwise} \end{cases},$$

where W_d is the $(d \times d)$ one level wavelet transform matrix, as explained in Step i, and I_d is the $(d \times d)$ identity matrix.

iv. For each level m, construct an $(N \times N)$ transformation matrix Ψ_m as

$$\Psi_m = \begin{bmatrix} D_1 & & & 0 \\ & D_2 & & \\ & & \ddots & \\ 0 & & & D_{2^{m-1}} \end{bmatrix}.$$

v. Calculate the OWP matrix as a concatenated filter

$$\Psi^\star = \Psi_L,\ \Psi_{L-1}, \ldots, \Psi_1.$$

The GOCS algorithm optimizes the basis $\Psi^\star$ to the PU signal $\mathbf{x}$, using Algorithms 1 and 2. After collecting the measurements $\mathbf{y}$ at the desired compression ratio m/N, GOCS then proceeds to find $\hat{\mathbf{x}} = \text{OMP}(\mathbf{y}, \Phi, \Psi^\star)$. After receiving all J measurement vectors at the FC, GOCCS reconstructs the measured signals by $\hat{\mathbf{X}} = \text{SOMP}(\mathbf{Y}, \Phi, \Psi^\star)$, where Φ is known a priori by the FC.

5. BLINDLY OPTIMIZED COMPRESSED SENSING

The genie-aided algorithms are described for theoretical understanding of the performance limits of the proposed approach. However, in practice, a sensing node cannot know the exact characteristics of the sensed signal. In this section, we propose a practical solution to this problem.

5.1. Proposed Blindly-optimized CCSS Algorithm

Since the measured signals are not known a-priori to the sensing nodes or the FC, the proposed genie-aided algorithms are modified to blindly optimize the sparsifying basis. In the proposed blindly optimized compressed sensing (BOCS) algorithm, the representation basis is optimized without any prior knowledge about the measured PU signal. The crux of the BOCS algorithm is to optimize the basis to an estimate of the wide-band measured signal $\hat{\mathbf{x}}$, instead of the actual measured signal. The BOCS algorithm estimates $\hat{\mathbf{x}}$ from the measurement vector $\mathbf{y}$ only, by signal reconstruction with a fixed sparsifying basis such as the FWP or the wavelet transform. Let W denote the FWP transform matrix, then for CS with the FWP transform (CS-WP), the estimated reconstructed signal is

$$\hat{\mathbf{x}}_W = \text{OMP}(\mathbf{y}, \Phi, W). \tag{9}$$

The BOCS algorithm optimizes the sparsifying basis $\Psi^\star$ to the estimated signal by

$$\Psi^\star = \arg_\Psi \min \mathcal{S}\left(\Psi^{-1}\hat{\mathbf{x}}_W\right), \tag{10}$$

where the OWP tree is found for $\hat{\mathbf{x}}_W$ with the CW algorithm and $\Psi^\star$ is found from the estimated OWP tree, as explained above for the genie-aided algorithms. The BOCS algorithm proceeds to reconstruct a better estimate of the measured signal from the measurement vector $\mathbf{y}$ using the optimized basis $\Psi^\star$, c.f., (6),

$$\hat{\mathbf{x}}_O = \text{OMP}(\mathbf{y}, \Phi, \Psi^\star). \tag{11}$$

For cooperative sensing, the FC deploys the following BOCCS algorithm to estimate the PU signal $\mathbf{x}$ from the measurement matrix $\mathbf{Y}$:

Algorithm 3 *Blindly Optimized Cooperative Compressed Sensing (BOCCS)*

i. $\hat{\mathbf{X}}_W = \text{SOMP}(\mathbf{Y}, \Phi, W)$, c.f., Section 3.2

ii. $\hat{\mathbf{x}}_W = \text{mean}(\hat{\mathbf{X}}_W)$

iii. $\Psi^\star = \arg_\Psi \min \mathcal{S}(\Psi^{-1}\hat{\mathbf{x}}_W)$, c.f., (10)

iv. $\hat{\mathbf{X}}_O = \text{SOMP}(\mathbf{Y}, \Phi, \Psi^\star)$

v. $\hat{\mathbf{x}}_O = \text{mean}(\hat{\mathbf{X}}_O)$.

Block diagrams of the proposed BOCS algorithm and the (secure) BOCCS algorithm are shown in Figure 2 and Figure 3, respectively.

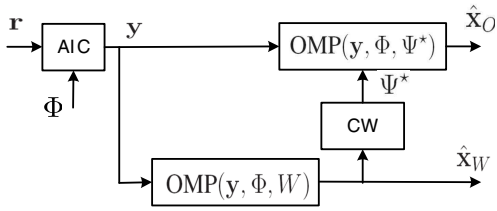

Figure 2. Block diagram of the proposed blindly-optimized compressed sensing (BOCS) algorithm.

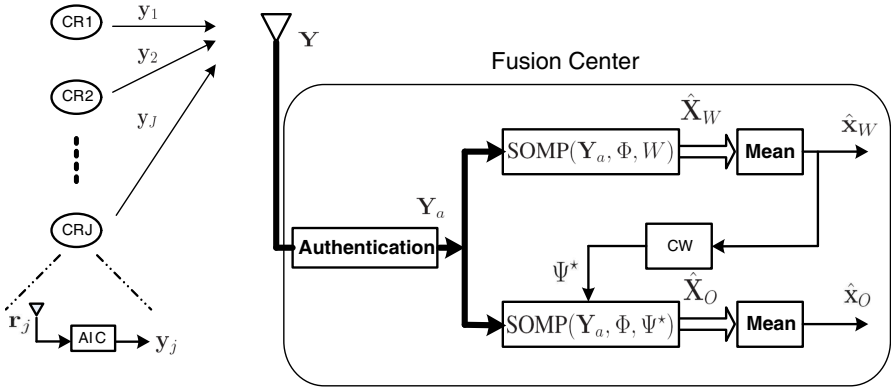

Figure 3. Block diagram of the proposed secure blindly-optimized cooperative CSS algorithm.

As shown in the simulation results of the next section, the proposed optimized CS algorithms require a smaller number of compressed measurements m to achieve the same detection performance as conventional CS schemes with fixed bases. A smaller m allows for cheaper sensing nodes with slower sampling rates and lower power consumption, where the hardware complexity and the power consumption of the analog-to-information converter circuit is almost linearly proportional to m [32]. In case of cooperative sensing, a smaller m also results in less required transmission power and bandwidth on the reporting channels to the FC. In practice, it is important that the

spectrum sensing nodes be cheap with low power consumption, as they may be battery operated, and it is acceptable to shift the complexity from the spectrum sensing nodes to the FC. The extra complexity from the optimization process of our proposed algorithms is performed at the FC, which has sufficient computing power. However, due to the smaller m, the SOMP reconstruction complexity at the FC is also reduced, as the time complexity of the SOMP algorithm is roughly $\mathcal{O}(J^2TmN)$ operations after T iterations, where T has the same order as the signal sparsity [28, 33].

5.2. Performance Analysis of Blindly-optimized CSS

The effectiveness of the genie-aided OWP (G-OWP) and the blind OWP (B-OWP) transforms in finding the most-sparse representation is evaluated. The system model of 2.2 is assumed. The Shannon entropy of (8) is averaged over 1000 random signals at different received PU SNRs, where all sub-bands are received with the same SNR, and compression ratio $m/N = 0.5$.

It is observed from the entropy measure in Figure 4 that the signal representation with the G-OWP or the B-OWP transforms is more sparse than with the conventional FWP transform. The wavelet transform results are eliminated since they have worse performance. Blind optimization results in a slight loss in sparsity compared to the genie optimized transform. For illustration purposes, a sampled PU signal and its corresponding sparse representations, assuming 10 dB

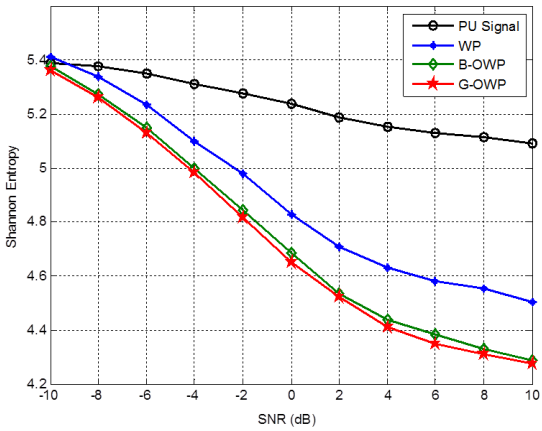

Figure 4. Sparsity of the proposed blind and genie-aided OWP transforms compared to that of the conventional FWP transform and the original PU signal.

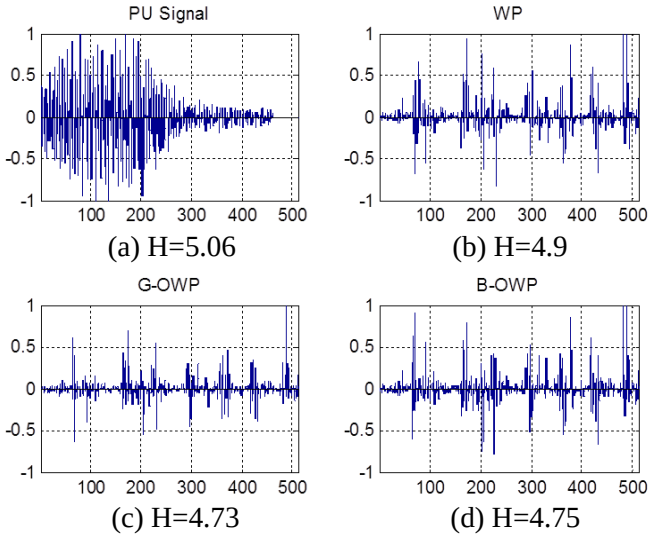

Figure 5. (a) PU signal. (b) Its sparse representations with the FWP. (c) G-OWP. (d) B-OWP transforms.

SNR and $m/N = 0.5$ are shown in Figure 5. The quoted entropy values also confirm that the B-OWP transform achieves significant sparsity gain over the conventional FWP transform.

To illustrate the accuracy in reconstructing the measured PU signal, the normalized mean square error (NMSE) in the reconstructed PU spectrum $\widehat{\mathbb{S}}_{\mathbf{x}}$ is analyzed at different measurement compression ratios, where

$$\text{NMSE} = \text{E}\left\{\frac{\|\mathbb{S}_{\mathbf{x}} - \widehat{\mathbb{S}}_{\mathbf{x}}\|^2}{\|\mathbb{S}_{\mathbf{x}}\|^2}\right\}, \tag{12}$$

E{.} denotes the expectation, and $\mathbb{S}_{\mathbf{x}}$ is the spectrum of the transmitted PU signal.

For Monte-Carlo simulations, the performance is averaged over different SNRs, where the PU signals are received at the sensing terminals with different SNRs on the four occupied channels, and respectively given by $[-10, -5, 0, 5]$ dB. The NMSE is evaluated for the conventional CS with FWP transform (CS-WP) and compared to that of the proposed BOCS and GOCS algorithms. Concurrently, the gain achievable by cooperation between the sensing nodes is analyzed. Hence, the performance with 10 cooperating spectrum sensing nodes is evaluated with CS-WP and compared to that of the proposed BOCCS and GOCCS algorithms. From Figure 6(a), it is observed that, at

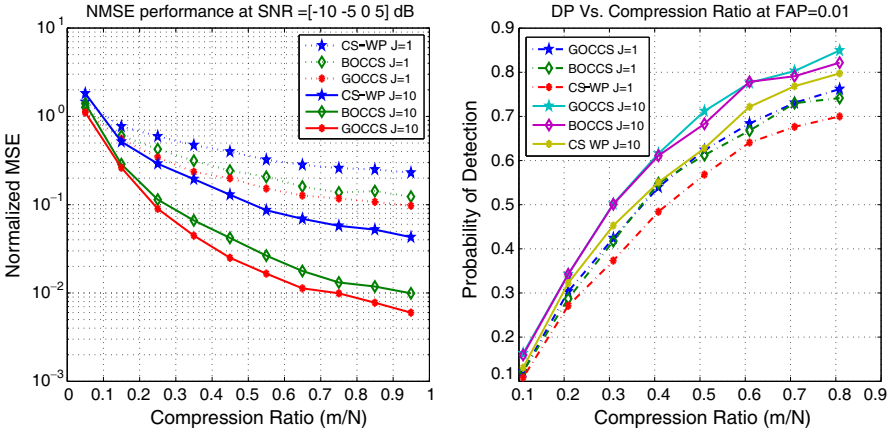

Figure 6. Comparison of proposed schemes with conventional scheme for individual and cooperative spectrum sensing with 10 cooperative nodes, for (a) the reconstruction normalized MSE and (b) PU detection reliability at different sensing rates.

any compression ratio, BOCS and BOCCS provide improvements in the PU signal reconstruction accuracy compared to CS-WP, along with a slight loss compared to the genie-aided algorithms. The gain from cooperation is also illustrated, where BOCCS achieves a ten percent NMSE at $m/N < 0.3$ with 10 cooperating nodes, but requires $m/N > 0.95$ to achieve the same NMSE with one sensing node only.

Complexity reduction by the optimized algorithms at the target $P_{\mathcal{F}} = 0.01$, as explained in Section 5.1, is demonstrated in Figure 6(b) by the reduction in the sensing rate m/N at the same detection probability.

The tradeoff between detection and false alarm probabilities is analyzed by the ROC curves in Figure 7, and it is concluded that the proposed optimized sensing algorithms are superior to conventional ones that deploy FWP transforms. The cooperative gain is shown in Figure 8(a), where detection performance is analyzed at a different number of cooperating nodes, at $m/N = 0.5$ and $P_{\mathcal{F}} = 0.01$. The effect of the received PU SNR on the reliability of the optimized CCSS algorithms is analyzed by evaluating the detection probability when the PU signal is received on the occupied channels with the same SNR, as shown in Figure 8(b). From the results shown in Figures 6(b)–8(b), it is observed that the proposed BOCCS consistently offers significant gains in PU protection by increasing the detection probability at other

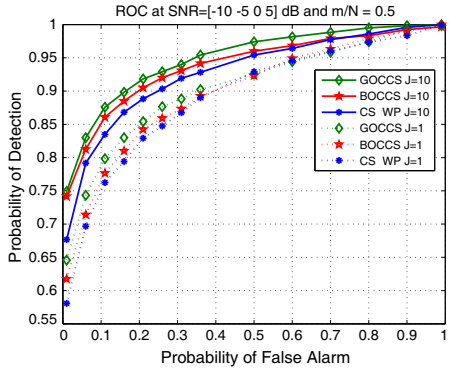

Figure 7. Comparison of the receiver operation characteristics of the proposed BOCCS and GOCCS with conventional CS-WP for individual and cooperative spectrum sensing.

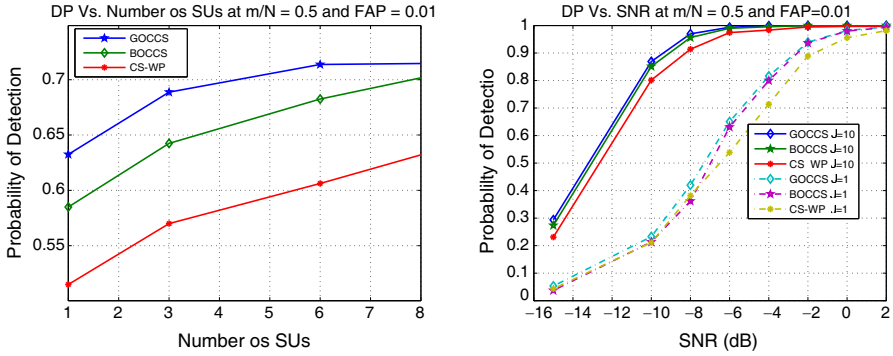

Figure 8. Probability of detection of proposed schemes versus (a) the number of cooperating nodes, (b) SNR at a target $P_{\mathcal{F}} = 0.01$.

fixed system parameters as false alarm probability, PU SNR, and compression ratio. Also, the degradation in incumbent user detection by the blindly-optimized algorithms, compared to the genie-aided algorithms, is not significant. It is also observed that significant gains can be achieved by cooperation between the sensing nodes, especially in practical scenarios with very low received PU SNRs.

To demonstrate spatial diversity gains, a CR network constituting of three spatially located nodes and a FC is considered. Depending on its location, each SU node receives the PU signal with different SNRs on the occupied channels. The received PU SNRs at the sensing

nodes SU_1, SU_2, and SU_3 are $[-1, -1, -6, -6]$ dB, $[0, 0, -5, -5]$ dB, and $[1, 1, -4, -4]$ dB, on the four occupied channels respectively. Figure 9(a) shows the ROC enhancement when deploying BOCCS with the 3 cooperating sensing terminals compared to single-terminal BOCS. The enhanced PU protection through cooperation illustrates that the proposed BOCCS scheme successfully incorporates the spatial diversity gains.

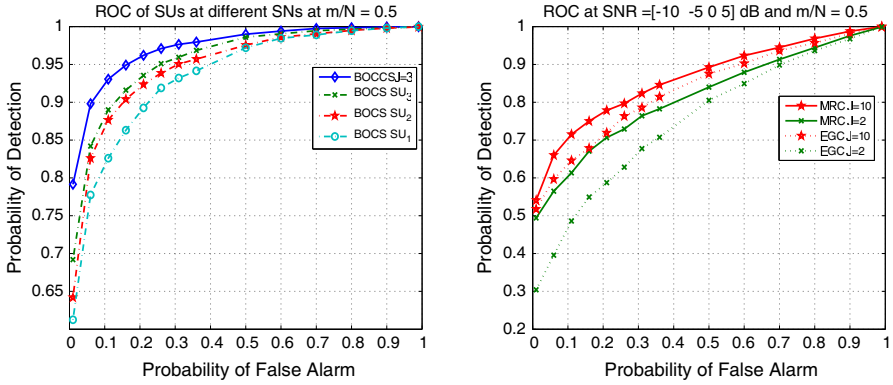

Figure 9. (a) Cooperative diversity gain showed (a) ROCs with 3 sensing nodes at $m/N = 0.5$ and different received SNRs, (b) ROC of BOCCS with maximal-ratio or equal-gain combining in case of non-ideal reporting channels.

In the previous results, an ideal reporting channel between the spectrum sensing nodes and the FC (base-station) was assumed. The cooperative combining gain of the proposed BOCCS algorithm is analyzed in case of a non-ideal reporting channel. The SNR of each reporting channel can be an indication of the distance between the spectrum sensing node and the FC. In case of equal gain combining, the measurement vectors are not scaled at the FC. The proposed cooperative CS algorithms are modified, to incorporate maximum ratio combining (MRC), where each measurement vector $\mathbf{y}_j$ is scaled by its reporting channel SNR γ_j, such that augmented measurement matrix at the FC is given by $\mathbf{Y} = \{\gamma_1\mathbf{y}_1, \gamma_2\mathbf{y}_2, \ldots, \gamma_J\mathbf{y}_J\}$.

A scenario of $J = 10$ spectrum sensing nodes with reporting SNRs from sensing terminals to the fusion center of $[1, -1, 3, -3, 5, -5, 7, -7, 10, -10]$ dB is assumed. The performance of the proposed BOCCS with MRC is compared to that of BOCCS with conventional equal gain combining (EGC) when the measurements are received at the FC from all spectrum sensing nodes ($J = 10$) or from only the first

two spectrum sensing nodes ($J = 2$). From Figure 9(b), the ROC curves show that the proposed MRC method significantly improves the detection performance, and the gains are more significant with a smaller number of cooperating nodes. In Figure 10, the performance of the proposed BOCCS, and GOCCS is compared to CS-WP, when MRC of the reported measurements is deployed. The gains of BOCCS are in agreement with the above results in case of ideal reporting channels.

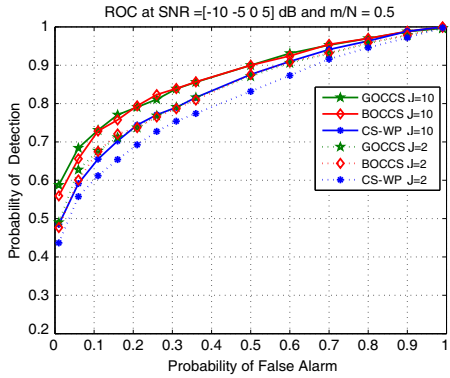

Figure 10. ROC comparisons of BOCCS, GOCCS, and CS-WP when deploying MRC over non-ideal reporting channels from sensing terminals to the fusion center.

6. SECURE COOPERATIVE COMPRESSED SPECTRUM SENSING

In this section, we consider the performance of a CCSS system when it is under attack from malicious users. Data falsification attackers may send random data as measurements to the FC, in order to corrupt the CR system and degrade the throughput performance of the PU. Alternatively, greedy attackers may deliberately send wrong measurement data to force the secondary system to refrain from utilizing the white spectrum spaces. Hence, improving the security of cooperative spectrum sensing systems is crucial to their success.

6.1. Proposed Secure BOCCS

To mitigate security attacks against CCSS systems, we propose an authentication mechanism that does not require extra overhead or complex computations, as in encryption-based methods, but is rather inherent to the compressed sensing system. Moreover, the proposed

secure CCCS scheme, does not significantly add extra complexity to the low-power low-cost CSS nodes. A block diagram of the proposed secure BOCCS (SBOCCS) algorithm is shown in Figure 3 and is described as follows:

Algorithm 4 *Secure Blindly Optimized Cooperative Compressed Sensing*

i. Each FC center shares its $m \times N$ sensing matrix Φ, or the random seed used to generate it, periodically, with its spectrum sensing nodes over a secure channel. Alternatively, proprietary algorithms, known only to the FC and the spectrum sensing nodes, can be used to generate and periodically change the sensing matrix Φ.

ii. For the sensing matrix Φ determined in step i, the FC calculates a decision threshold by

$$\zeta_a = a\frac{\left\|\Phi^T\Phi\mathbf{1}_N\right\|}{\|\Phi\mathbf{1}_N\|},$$

where $\mathbf{1}_N$ is the $1\times N$ all-one vector normalized to unit energy, $0 < a \leq 1$ is a damping factor, and for any vector $\mathbf{x} = [x_1, x_2, \ldots, x_N]$, $\|\mathbf{x}\| = \sqrt{\sum_{i=1}^{N} x^2}$ is the l_2 norm of $\mathbf{x}$.

iii. Following CCSS, each sensing node transmits its measurement vector $\mathbf{y}_j$ to the FC. On the contrary, malicious nodes will send random measurements, or alternatively measurements using another random sensing matrix $\tilde{\Phi}$, to the FC.

iv. The FC correlates each received measurement vector $\mathbf{y}_j$ with the predetermined measurement matrix Φ to calculate the correlation coefficient

$$\rho_j = \frac{\left\|\Phi^T\mathbf{y}_j\right\|}{\|\mathbf{y}_j\|}.$$

v. The FC constructs the authenticated set of measurement vectors $\mathcal{A}$, where each received vector $\mathbf{y}_j$ is authenticated by

$$\begin{array}{ll}\mathbf{y}_j \in \mathcal{A}, & \text{if } \rho_j \geq \zeta_a \\ \mathbf{y}_j \notin \mathcal{A}, & \text{if } \rho_j < \zeta_a.\end{array}$$

vi. The authenticated measurement matrix $\mathbf{Y}_a$ is constructed by augmenting all authenticated measurement vectors in $\mathcal{A}$.

vii. The BOCCS algorithm, as explained by Algorithm 3, is operated on the authenticated measurement matrix $\mathbf{Y}_a$ such that the first estimate of the PU signal using the FWP transform is calculated as $\hat{\mathbf{X}}_W = \text{SOMP}(\mathbf{Y}_a, \Phi, W)$, and used to optimize $\Psi^\star$. Hence, the measured PU signal is estimated by the reconstruction $\hat{\mathbf{x}}_O = \text{mean}(\text{SOMP}(\mathbf{Y}_a, \Phi, \Psi^\star))$.

The correlation coefficient of step iv is normalized by the norm of the received signal to factor out different measured signal energies, and thus be a characteristic of the measurement matrix Φ only. The correlation threshold of step ii is calculated once off-line, and thus does not add to the running complexity. This threshold is derived by observing that $\mathbf{y}_j = \Phi \mathbf{r}_j$, then the correlation coefficient for the jth sensing node can be written as

$$\rho_j = \frac{\left\| \Phi^T \Phi \mathbf{r}_j \right\|}{\| \Phi \mathbf{r}_j \|}. \tag{13}$$

Hence, the correlation threshold is calculated by assuming a flat received signal $\mathbf{r}_j = \mathbf{1}_N$. The damping factor a is a tunable parameter, where a larger a is more conservative and provides more security, at the expense of discarding measurements from trustful nodes, and a smaller a is more aggressive and is more likely to incorporate measurements from malicious users.

The proposed authentication procedure does not require any extra complexity (as encryption) from the spectrum sensing nodes, and does not require any extra communication overhead. SBOCCS only requires an extra correlation step at the FC. However, the gains from this simple authentication scheme can be significant, as shown in the following sub-section.

6.2. Performance Analysis of SBOCCS

A test scenario with 10 trustful secondary user sensing terminals and 10 malicious users is considered. The sensing terminals transmit their measurements of the PU signal, using the predetermined measurement matrix, to the FC. On the other hand, the malicious users transmit measurements of a wrong signal using a different random measurement matrix. While SBOCCS attempts to reconstruct the measured PU signal using the authenticated measurements only, BOCCS attempts to reconstruct the PU signal with all $J = 20$ received measurements.

To verify the proposed correlation threshold, the histogram of the correlation coefficients ρ_j with all (trustful and malicious) measurements is calculated over 2000 different statistics. The histogram in Figure 11 shows two different peaks, for the malicious user (MU) and trustful SU nodes. The expected threshold $\mathrm{E}\{\zeta_a\}$ over the different statistics is also shown for different values of the damping factor a. The suggested correlation threshold with $a = 0.91$ satisfies the authentication criterion

$$\rho_{\mathrm{MU}} < \zeta_a \leq \rho_{\text{trustful SU}}. \tag{14}$$

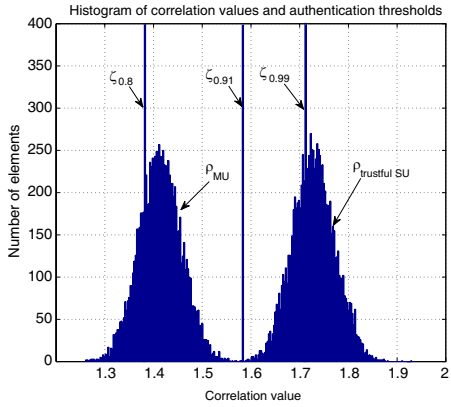

Figure 11. Histogram of the correlation coefficients with received measurements and the suggested thresholds of the proposed security authentication system.

It is also verified that $a = 0.99$ is more conservative and $a = 0.8$ results in accepting measurements from malicious users.

The effectiveness of the proposed authentication scheme is tested by comparing the ROC curves of BOCCS with those of SBOCCS. The remaining simulation parameters are similar to those used in Figure 7. The results of Figure 12 show that SBOCCS, with $a = 0.91$ achieves the near optimal performance with no malicious users (BOCCS, 0 MUs, $J = 10$). The effect of incorporating the malicious measurements (BOCCS, 10 MUs, $J = 20$) is shown through the decreased $P_{\mathcal{D}}$

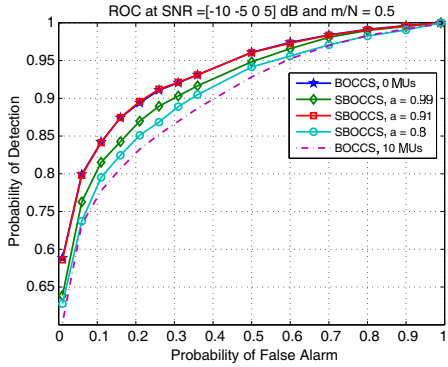

Figure 12. ROC performance of proposed SBOCCS algorithms in presence of malicious users.

at the same $P_{\mathcal{F}}$, or alternatively the higher $P_{\mathcal{F}}$ at the same $P_{\mathcal{D}}$. The results also imply that deploying a more conservative threshold ($a = 0.99$), which results in discarding some trustful spectrum sensing measurements, yields better performance than deploying a more aggressive threshold ($a = 0.8$), which results in utilizing false measurements in the reconstruction process.

7. CONCLUDING REMARKS

In this work, novel compressed spectrum sensing algorithms are proposed for enhanced incumbent user protection in cognitive radio systems, and improved security against malicious attacks. Different from conventional algorithms that used fixed sparsifying bases for sensing, this work optimizes the sparsifying bases to the sensed signal. This optimization is done blindly and does not require any knowledge about the characteristics of the sensed signal, which are not known in practical cognitive radio systems. The optimized compressed sensing algorithms were proposed for both single-terminal sensing and centralized cooperative sensing. Furthermore, optimal combining of compressed measurements from different sensing terminals is shown to provide spatial diversity gains. A simple, yet effective, authentication algorithm is proposed to improve the security of cooperative compressed sensing algorithms against malicious data-falsification attacks. The results show that the proposed spectrum sensing algorithms have improved incumbent user detection, require sensing terminals with lower hardware complexity and power consumption, require less communication overhead for cooperative sensing, and have improved protection against adversary attacks.

ACKNOWLEDGMENT

This work is partially supported by the Missions Department of the Egyptian Ministry of Higher Education (MOHE).

REFERENCES

1. Federal Communications Commission, et al., "Unlicensed operation in the TV broadcast bands," *ET Docket*, No. 04-186, 2004.
2. Federal Communications Commission, "Notice of proposed rule making and order: Facilitating opportunities for flexible, efficient, and reliable spectrum use employing cognitive radio technologies," *ET Docket*, No. 03-108, 73, 2005.

3. IEEE, "IEEE Std. 802.22-2011, IEEE standard for wireless regional area networks part 22: Cognitive wireless RAN medium access control (MAC) and physical layer (PHY) specifications: Policies and procedures for operation in the TV bands," 2011.
4. Yucek, T. and H. Arslan, "A survey of spectrum sensing algorithms for cognitive radio applications," *IEEE Communications Surveys & Tutorials*, Vol. 11, No. 1, 116–130, 2009.
5. Haykin, S., "Cognitive radio: Brain-empowered wireless communications," *IEEE Journal on Selected Areas in Communications*, Vol. 23, No. 2, 201–220, 2005.
6. Urkowitz, H., "Energy detection of unknown deterministic signals," *Proceedings of the IEEE*, Vol. 55, No. 4, 523–531, 1967.
7. Sahai, A. and D. Cabric, "Spectrum sensing: Fundamental limits and practical challenges," *Proc. IEEE International Symposium on New Frontiers in Dynamic Spectrum Access Networks (DySPAN)*, 2005.
8. Donoho, D., "Compressed sensing," *IEEE Transactions on Information Theory*, Vol. 52, No. 4, 1289–1306, Apr. 2006.
9. Candès, E. and M. Wakin, "An introduction to compressive sampling," *IEEE Signal Processing Magazine*, Vol. 25, No. 2, 21–30, 2008.
10. La, C. and M. Do, "Signal reconstruction using sparse tree representation," *Proc. Wavelets XI at SPIE Optics and Photonics*, San Diego, 2005.
11. Peyré, G., "Best basis compressed sensing," *Scale Space and Variational Methods in Computer Vision*, 80–91, 2007.
12. Liu, J., C. Z. Han, X. H. Yao, and F. Lian, "Compressed sensing based track before detect algorithm for airborne radars," *Progress In Electromagnetics Research*, Vol. 138, 433–451, 2013.
13. Wei, S.-J., X.-L. Zhang, J. Shi, and K.-F. Liao, "Sparse array microwave 3-D imaging: Compressed sensing recovery and experimental study," *Progress In Electromagnetics Research*, Vol. 135, 161–181, 2013.
14. Tian, Z. and G. Giannakis, "Compressed sensing for wideband cognitive radios," *IEEE International Conference on Acoustics, Speech and Signal Processing, ICASSP 2007*, Vol. 4, IV-1357–IV-1360, Apr. 2007.
15. Yu, Z., S. Hoyos, and B. Sadler, "Mixed-signal parallel compressed sensing and reception for cognitive radio," *IEEE International Conference on Acoustics, Speech and Signal Processing, ICASSP 2008*, 3861–3864, Apr. 2008.

16. Polo, Y., Y. Wang, A. Pandharipande, and G. Leus, "Compressive wide-band spectrum sensing," *IEEE International Conference on Acoustics, Speech and Signal Processing, ICASSP 2009*, 2337–2340, Apr. 2009.
17. Wang, Y., Z. Tian, and C. Feng, "A two-step compressed spectrum sensing scheme for wideband cognitive radios," *IEEE Global Telecommunications Conference GLOBECOM 2010*, 1–5, IEEE, 2010.
18. Wang, Y., A. Pandharipande, Y. Polo, and G. Leus, "Distributed compressive wide-band spectrum sensing," *Information Theory and Applications Workshop*, 178–183, IEEE, 2009.
19. Stevenson, C., G. Chouinard, Z. Lei, W. Hu, S. Shellhammer, and W. Caldwell, "IEEE 802.22: The first cognitive radio wireless regional area network standard," *IEEE Communications Magazine*, Vol. 47, No. 1, 130–138, 2009.
20. Akyildiz, I., B. Lo, and R. Balakrishnan, "Cooperative spectrum sensing in cognitive radio networks: A survey," *Physical Communication*, 40–62, 2010.
21. Li, Z., F. R. Yu, and M. Huang, "A cooperative spectrum sensing consensus scheme in cognitive radios," *IEEE INFOCOM 2009*, 2546–2550, IEEE, 2009.
22. Tian, Z., E. Blasch, W. Li, G. Chen, and X. Li, "Performance evaluation of distributed compressed wideband sensing for cognitive radio networks," *11th International Conference on Information Fusion 2008*, 1–8, IEEE, 2008.
23. Farrag, M., M. El-Khamy, and M. El-Sharkawy, "Secure cooperative blindlyoptimized compressive spectrum sensing for cognitive radio," *29th National Radio Science Conference (NRSC)*, 533–540, IEEE, 2012.
24. Chen, R., J. Park, Y. Hou, and J. Reed, "Toward secure distributed spectrum sensing in cognitive radio networks," *IEEE Communications Magazine*, Vol. 46, No. 4, 50–55, 2008.
25. Rawat, A., P. Anand, H. Chen, and P. Varshney, "Collaborative spectrum sensing in the presence of Byzantine attacks in cognitive radio networks," *IEEE Transactions on Signal Processing*, Vol. 59, No. 2, 774–786, 2011.
26. Coifman, R. and M. Wickerhauser, "Entropy-based algorithms for best basis selection," *IEEE Transactions on Information Theory*, Vol. 38, No. 2, 713–718, 1992.
27. Laska, J., S. Kirolos, Y. Massoud, R. Baraniuk, A. Gilbert, M. Iwen, and M. Strauss, "Random sampling for analog-to-

information conversion of wideband signals," *IEEE Dallas/CAS Workshop on Design, Applications, Integration and Software*, 119–122, IEEE, 2006.

28. Tropp, J. A., A. C. Gilbert, and M. J. Strauss, "Algorithms for simultaneous sparse approximation. Part I: Greedy pursuit," *Signal Processing*, Vol. 86, No. 3, 572–588, 2006.
29. Farrag, M., M. El-Khamy, and M. El-Sharkawy, "Optimized bases compressive spectrum sensing for wideband cognitive radio," *IEEE 22nd International Symposium on Personal Indoor and Mobile Radio Communications (PIMRC)*, 305–309, IEEE, 2011.
30. Farrag, M., M. El-Khamy, and M. El-Sharkawy, "A blindly optimized compressive sensing receiver for cognitive radio," *IEEE International Conference on Consumer Electronics (ICCE)*, 174–177, IEEE, 2012.
31. Hurley, N. and S. Rickard, "Comparing measures of sparsity," *IEEE Transactions on Information Theory*, Vol. 55, No. 10, 4723–4741, 2009.
32. Chen, F., A. P. Chandrakasan, and V. M. Stojanovic, "Design and analysis of a hardware-efficient compressed sensing architecture for data compression in wireless sensors," *IEEE Journal of Solid-State Circuits*, Vol. 47, No. 3, 744–756, 2012.
33. Goodman, J., K. Forsythe, and B. Miller, "Efficient reconstruction of blocksparse signals," *IEEE Statistical Signal Processing Workshop (SSP)*, 629–632, 2011.